

## Angular Size Measurements Of Mira Variable Stars At 2.2 $\mu\text{m}$ . II

G. T. van Belle<sup>1</sup>

R. R. Thompson

M. J. Creech-Eakman<sup>2</sup>

*Jet Propulsion Laboratory, California Institute of Technology, Pasadena, CA 91109*

### ABSTRACT

We present angular size measurements of 22 oxygen-rich Mira variable stars. These data are part of a long term observational program using the Infrared Optical Telescope Array (IOTA) to characterize the observable behavior of these stars. Complementing the infrared angular size measurements, values for variable star phase, spectral type, bolometric flux and distance were established for stars in the sample; flux and distance led to values for effective temperature ( $T_{EFF}$ ), and linear radius, respectively. Additionally, values for the  $K - [12]$  color excess were established for these stars, which is indicative of dusty mass loss. Stars with higher color excess are shown to be systematically  $120 R_{\odot}$  larger than their low color excess counterparts, regardless of period. This analysis appears to present a solution to a long-standing question presented by the evidence that some Mira angular diameters are indicative of first overtone pulsation, while other diameters are more consistent with fundamental pulsation. A simple examination of the resultant sizes of these stars in the context of pulsation mode is consistent with at least some of these objects pulsating in the fundamental mode.

*Subject headings:* stars: variables: Mira, infrared: stars, stars: fundamental parameters, stars: late-type, techniques:interferometric

---

<sup>1</sup>Email address: gerard@huey.jpl.nasa.gov.

<sup>2</sup>Caltech/JPL Postdoctoral Scholar.

## 1. Introduction

The recent development of interferometric methods at optical and infrared wavelengths has provided the astronomical community with more than an order of magnitude increase in spatial resolution over direct imaging techniques. Using the Infrared Optical Telescope Array (IOTA, see Carleton et al. (1994) and Dyck et al. (1995)) and the Palomar Testbed Interferometer (PTI, see Colavita et al. (1999)), we have been conducting a program of high resolution, K band observations of Mira variable stars. Previous IOTA results have been presented for both oxygen-rich Miras (van Belle et al. 1996), and carbon & S-type Miras and non-Mira S-type stars (van Belle et al. 1997).

Mira variables figure prominently in our observing strategy, since these stars are large and bright at infrared wavelengths. Using crude estimates of surface temperatures and the observed total fluxes it is estimated that more than 100 such stars have black body angular diameters in excess of 2 milliarcseconds (mas), easily resolvable targets for the current generation of Michelson interferometers. The 22 stars reported herein represent a significant collection of angular sizes to be added to the literature, roughly doubling the number of sizes available. This large sample allows for a more detailed analysis of the behavior of these stars.

Recent investigations of Mira variables have attempted to resolve important questions regarding the pulsation mode, mass loss and evolution of these stars. The pulsation mode remains a currently-unresolved issue; the promise of high-resolution interferometric methods to firmly resolve this question is hampered by conflicts between distance-determination methods. Initial studies of these stars in the visible (Haniff, Scholz & Tuthill 1995; Lattanzi et al. 1997; Burns et al. 1998; Young et al. 2000), and infrared (van Belle et al. 1996, 1997; Perrin et al. 1999; Hofmann et al. 2002; Thompson, Creech-Eakman & van Belle 2002), have yet to provide conclusive evidence in favor of fundamental versus first overtone pulsation mode, although a deeper understanding of these complex and dynamic stellar atmospheres is beginning to emerge as a direct result of these investigations.

Studies attempting to derive distances to Miras, independent of assumptions about pulsation mode, fail to reach agreement on the subject. Whitelock & Feast (2000), utilizing parallax data from the Hipparcos satellite to derive a K-band period-luminosity relation, which, in conjunction with Mira angular size data and published model atmospheres, they find to indicate a common first overtone mode for most Miras. The resultant LMC distance modulus Whitelock and Feast derive is  $18.64 \pm 0.14$ , which is consistent with similar determinations utilizing Cepheids (Groenewegen 2000) but in conflict with recent LMC distances as indicated by eclipsing binaries (Nelson et al. 2000; Ribas et al. 2000; Groenewegen & Salaris 2001) that favor smaller distance modulus values of  $18.46 \pm 0.06$  or less. In contrast to that

investigation, Alvarez & Mennessier (1997), utilizing TiO and VO band strengths, arrive at radii and temperatures that favor fundamental pulsations. This finding is in agreement with the group of Wood et al. (1999); Wood (2000), which examines Mira period ratios found in MACHO data to argue strongly in favor of fundamental mode. Depending upon initial assumptions, models supporting both fundamental mode pulsation (Willson & Hill 1979; Hill & Willson 1979; Wood 1990) and first overtone pulsation (Wood 1974; Tuchman, Sack & Barkat 1979; Perl & Tuchman 1990) have been constructed, in certain cases, the pulsation mode itself is a free parameter (Hofmann, Scholz & Wood 1998).

It is by means of direct observation of the angular sizes of Mira variables that we may be able to provide unique insight into these questions. Additional information in the form of bolometric flux estimates will yield further information, such as effective temperature, which remains a poorly established quantity for this class of stars. Also, our angular size measurements and derived quantities have implications regarding the nature of mass loss and evolution among Mira variables.

Carbon-rich, oxygen-rich and S-type Miras were all observed at IOTA and the Palomar Testbed Interferometer (PTI) as a part of our ongoing high resolution program; in this paper we present only the observations of the oxygen-rich variety observed at IOTA. Observations at IOTA using the related FLUOR experiment are not considered in this article as part of the data set (Perrin et al. 1999), although they are in agreement with our conclusions, particularly that of fundamental mode pulsation for Miras (Hofmann et al. 2002). Operations at IOTA that produced these results are discussed in §2, detailing source selection and observation. In §3 the procedures used in establishing the stellar parameters for the stars observed are discussed; the parameters include phase, spectral type, bolometric flux, angular size, effective temperature and linear radius. These parameters are in turn examined for significant interrelationships in the discussion of §4.

## 2. Observations

The data reported in this paper were obtained in the  $K$  band ( $\lambda = 2.2 \mu\text{m}$ ,  $\Delta\lambda = 0.4 \mu\text{m}$ ) at IOTA, using the 21 and 38 meter baselines. Use of IOTA at  $2.2 \mu\text{m}$  to observe Mira variables offers three advantages: First, effects of interstellar reddening are minimized, relative to the visible ( $A_K = 0.11A_V$ ; Mathis (1990)); Second, the effects of circumstellar emission are minimized shortward of  $10 \mu\text{m}$  (Rowan-Robinson & Harris 1983), and; Third, the  $K$  band apparent uniform-disk diameter of Mira variables has in the past been expected to be close to the  $\tau = 1$  Rosseland mean photospheric diameter (see the discussions in §3.3 and §4). The interferometer, detectors and data reduction procedures have been described

more fully by Carleton et al. (1994) and Dyck et al. (1995). As was previously reported in these papers, starlight collected by the two 0.45 m telescopes is combined on a beam splitter and detected by two single element InSb detectors, resulting in two complementary interference signals. The optical path delay is mechanically driven through the white light fringe position to produce an interferogram with fringes at a frequency of 100 Hz. Subsequent data processing locates the fringes in the raw data and filters out the low and high frequency noise with a square filter 50 Hz in width. Recent software and hardware upgrades to the computers driving the interferometer and collecting the data have resulted in a improved data collection rate to 1500-2000 fringe packets per night. On the best nights we can observe 20 science sources and an equal number of calibrators.

Observations of target objects are alternated with observations of unresolved calibration sources to characterize slight changes in interferometer response (no more than a few percent), due to both seeing and instrumental variations. Raw visibilities are determined from the amplitude of the interferogram at the white light fringe position, normalized by the incoherent flux from the star. An estimate of the noise is obtained from a similar measurement made in the data outside the region of coherence; the noise estimate is used in obtaining a weighted average of the visibility data, which is typically taken in sets of 50 interferograms. The raw visibilities of the target objects are then calibrated by dividing them by the measured visibilities of the calibration sources, using the calibration sources as samples of the interferometer’s point response. Calibration sources were selected from  $V$  band data available in The Bright Star Catalog, 4th Revised Edition (Hoffleit 1982) and  $K$  band data in the Catalog of Infrared Observations (Gezari et al. 1993), based upon angular sizes calculated from estimates of bolometric flux and effective temperature; calibration source visibility was selected to be at least 90% and ideally greater than 95%, limiting the effect of errors in calibrator visibility to a level substantially below measurement error.

Mira variables observed for this paper were selected based upon a number of criteria. Stars needed to be bright enough in  $V$  and  $K$  to be detected by both the star trackers and the InSb detectors; the current limits of the IOTA interferometer dictate  $V < 8.0$  mag and  $K < 5$  mag (though for observations at all airmasses and seeing conditions, we require  $K < 2.5$  mag). The Mira variables needed to be at a declination accessible to the mechanical delay available for a given evening. This is because the difference in delay between the two apertures, which can range from -30 m to +20 m, depends upon source declination and hour angle. Since only 4.6 m of this range is accessible at any time, observing is constrained to a specific declination bin about 10 deg wide on any given night. The stars also needed to be of sufficient estimated angular size to be resolved by IOTA. Mira phase was not a factor in target selection; hence, our targets represent Miras at a variety of phases, from visible light maximum to minimum.

Twenty-two oxygen-rich Mira variables were observed at IOTA during four observing runs in March, May/June, October of 1996, and July of 1997. The visibility data for the two detector channels have been averaged and are listed in Table 1, along with the date of the observation, the interferometer projected baseline, the stellar phase and the derived uniform disk angular size; the latter two points are discussed further in §3. In our experience with the IOTA interferometer, Dyck et al. (1996) has demonstrated that the night-to-night RMS fluctuations in visibility data generally exceed the weighted statistical error from each set of interferograms; we have characterized these fluctuations and use the empirical formula  $\sigma_V = \pm 0.051/\sqrt{N}$  (number of nights) to assign the “external” error. The interested reader should see Dyck et al. (1996) for a more complete discussion. Finally, visibility data were fit to uniform disk models to obtain an initial angular size  $\theta_{UD}$ . These uniform disk diameters and their estimated errors, derived from the uncertainty in the visibilities, are also listed in Table 1.

We note that typically a single point was utilized in calculating the uniform disk diameter  $\theta_{UD}$ . For the stars in our sample, the visibility data were all at spatial frequencies,  $x$ , shortward of the first zero of the uniform disk model,  $|2J_1(x)/x|$ , where  $x = \pi\theta_{UD}B/\lambda$ . Haniff, Scholz & Tuthill (1995) noted that the uniform disk model was not a particularly good model for visible-light data for Mira variables; rather, the data were a better fit to a simple Gaussian. Although we do not currently have multiple spatial frequency data for any Mira variables, our naive expectation as followed in van Belle et al. (1996, 1997) was that the departures from a uniform disk model will not be as great at  $2.2 \mu\text{m}$  as it is at visible wavelengths. This expectation appears to be borne out by comparisons of the data for R Aqr in van Belle et al. (1996) with the observations of Tuthill et al. (2000), although as we shall see in §4, this may not be entirely accurate. Thus, initially we will assume that to first order, a uniform disk model will also fit the Mira data; a slight correction to the derived angular sizes to account for this assumption will be discussed in §3.3. In this case, a single spatial frequency point will uniquely and precisely determine the angular diameters for visibilities in the approximate range  $0.25 \geq V \geq 0.75$ . As we shall see in §4, there is evidence this approach does not properly account for the deviation of a uniform disk size from the Rosseland mean diameter. Properly examining this point may only be addressed by detailed multiple spatial frequency observations of the visibility curves.

### 3. Stellar Parameters

#### 3.1. Phase

The phases of the Mira variables observed were established by means of two sources, following the procedure outlined in van Belle et al. (1996, 1997). Periods were initially obtained from The General Catalog of Variable Stars, 4th Edition (GCVS, Kholopov et al. (1988)). However, since the zero phase date in the GCVS at the epoch of the observations was no less than 11 cycles old for our sample stars, visual brightness data available from the Association Francaise des Observateurs d’Etoiles Variables (AFOEV) was utilized in estimating a recent zero phase date (Schweitzer 1998).

As an additional cross-check, Fourier analysis (as discussed in Scargle (1982) and Horne & Baliunas (1986)) of the AFOEV data also provided period information, but using light curve data which was more recent than that found in the GCVS. The periods from the GCVS and the AFOEV analysis agreed at the 1% level, corresponding to an average difference in period of  $1 \pm 4$  days. With the agreement in periods, the zero phase estimate was the larger uncertainty in phase determination, although this uncertainty was still small, averaging 6d. Periods, determined from Fourier analysis of the AFOEV data, and phases for each of the Mira variables are presented in Table 1.

#### 3.2. Spectral Type & Bolometric Flux

Bolometric fluxes ( $F_{BOL}$ ) of the Mira variable stars were estimated from a relationship between  $F_{BOL}$  and  $2.2 \mu\text{m}$  flux ( $F_K$ ), as established by Dyck, Lockwood & Capps (1974). In order to obtain bolometric fluxes,  $K$  magnitudes were first estimated from the incoherent (off-fringe) flux levels present in the IOTA data. We obtained our standard star photometric calibrations using the  $K$  band measurements found in the Two Micron Sky Survey (Neugebauer & Leighton 1969) for our non-variable point-response calibration sources. Cross-calibrator comparison of the published versus measured values for  $m_K$  indicates the IOTA photometry is consistent with the previous measures, with uncertainty being dominated by measurement scatter. No airmass corrections were applied since the calibrators were observed at nearly identical airmasses as the Mira variables. In all cases the bolometric fluxes were obtained from the absolute  $K$  fluxes through the observed relation

$$\log(F_K/F_{BOL}) = 0.017 \times (V - K) - 0.74 \quad (1)$$

which is the mean relationship derived from Dyck, Lockwood & Capps (1974) for spectral types M5-M10. A 15% error bar was assigned to the resultant  $F_{BOL}$  values, which is con-

sistent with more detailed  $F_{BOL}$  estimations done by Whitelock & Feast (2000). We note that the  $\log(F_K/F_{BOL})$  - spectral type relationship also has a firm theoretical basis and may be seen in the “infrared flux method” calculations carried out by Blackwell & Lynas-Gray (1994). No reddening corrections were applied to obtain the bolometric fluxes. These were deemed unnecessary since the typical magnitude of the corrections will be  $\Delta m_K < 0.10$  mag (calculated from the empirical reddening determination of Mathis, 1990, and from the  $A_V$  values given for local Miras in Whitelock et al. 2000), is less than the RMS K band error,  $\Delta m_K = 0.15$  mag.

In contrast to our previous paper on this subject (van Belle et al. 1996), spectral types were *not* inferred from the mean observation data of Lockwood & Wing (1971) or Lockwood (1972). We note instead that over the range of spectral types in question (M5-M9.8), the  $\log(F_K/F_{BOL})$  vs.  $V - K$  relationship is nearly flat, making the determination of  $F_{BOL}$  robust despite possible errors in  $V - K$  color. An uncertainty of one full magnitude in  $V - K$  results in only a 4% difference in the determined  $F_{BOL}$ ; we shall see in §3.4 that this results in a negligible difference in the determined effective temperature. The errors in the  $K$  magnitudes are the standard deviations of the individual measurements on a given night. From the observed scatter in the  $F_K/F_{BOL}$  relationship we estimate an rms error of  $\pm 13\%$  in  $F_{BOL}$  from the use of the  $K$  magnitude; we estimate a further uncertainty of  $\pm 5\%$  in the absolute calibration (Blackwell & Lynas-Gray 1994). The estimated error for  $F_{BOL}$  in Table 2 is the quadrature sum of these contributions of 15%.

### 3.3. True Angular Diameter

In order to estimate effective temperatures, the uniform disk diameters in Table 1 needed to be converted to stellar diameters corresponding to the non-uniform extended atmospheres of the Mira variables. We used the model Mira atmospheres discussed in Hofmann, Scholz & Wood (1998)[HSW98]. We note that the HSW98 models did not account for the time for both shock compressed material and material expanding between shocks to return to radiative equilibrium. These regions, with  $T > T_{RadEq}$  and  $T < T_{RadEq}$ , respectively, can alter the brightness distribution profile and consequently alter the ‘true’ angular sizes derived from the uniform disk (UD) diameters. Rather, HSW98 follows Bessel, Scholz & Wood (1996) in the semi-empirical adoption of an equilibrium temperature just behind the shock front. Dynamical atmosphere calculations have the potential to resolve these concerns (Bowen 1988; Bowen & Willson 1991); however, center-to-limb brightness profiles are not yet available for such calculations. The missing physics in the models has the potential to make for poor agreement between angular sizes derived at different wavelength bands.

Noting these concerns, here we shall use the HSW98 models as a sufficient expectation of the intensity distribution across the disk of a Mira variable to proceed with our analysis. Fortunately, as illustrated in HSW98, the K band is a particularly forgiving bandpass in which to work, and the differences between UD diameters and the Rosseland mean radiating surface is potentially small. Examining all of the HSW98 models, four of the six models (series Z, D, E and O) were seen as most representative of the parameters that matched the Miras observed; specifically, examining the bolometric flux variations of the local Miras as seen in Whitelock & Feast (2000), the average  $\Delta m_{BOL} = 0.73 \pm 0.25$ , which compares well with the bolometric flux variations seen in those four models in HSW98. For those models, the rms difference between a uniform disk fit and the Rosseland mean diameter is  $1.00 \pm 0.04$ , which we shall use as a scaling factor from which Rosseland angular sizes can be derived from K band UD diameters. Within the context of a unit scaling factor, the main quantitative impact upon the Rosseland mean diameter from the UD diameter is the slight increase in error due to the uncertainty in scaling factor. A scaling factor equal to unity is consistent with expectation that near-infrared uniform disk diameters should be reasonable as direct indicators of the true photospheric diameters of Mira variables (Willson (1986)), although contrasting with the possibility that extended atmospheric constituents might affect the apparent stellar size (Bedding et al. (2001)). As we shall see in §4, this appears to be more than a mere possibility.

In our previous article on Miras observed at IOTA (van Belle et al. 1996), we utilized a phase-dependent scaling as derived from Scholz & Takeda (1987), ranging from 0.98 at maximum light to 1.11 at minimum light. For this article, we decided to utilize a constant scaling in order to increase our sensitivity to true size and temperature variations, rather than variations derived from varying scaling factors. Our UD diameters from van Belle et al. (1996) were re-scaled using the  $1.00 \pm 0.04$  value above as well.

We also note that some consideration was given to the possibility of departures from spherical symmetry in these variable stars. As has been observed in visible light observations of Mira variables (Karovska et al. 1991; Haniff et al. 1992; Wilson et al. 1992; Weigelt et al. 1996; Tuthill et al. 1999a), these stars can be considerably elongated, possessing up to a 20% difference between semi-major and semi-minor axes, although this appears to diminish at  $1.0 \mu\text{m}$  (Hofmann et al. 2000). Similar observations at  $2.2 \mu\text{m}$  have indicated that this elongation is potentially present in the near-IR as well, with asymmetries of up to 25% (Tuthill et al. 2000; Thompson, Creech-Eakman & Akeson 2002). Such K band asymmetries potentially could be explained in terms of high-layer water or other molecular contamination seen to be present in models at certain combinations of parameters and phase cycle (Bedding et al. 2001; Scholz 2001), and are consistent with recent observations of Miras using  $0.1 \mu\text{m}$  bands across the K band window (Thompson, Creech-Eakman & van Belle 2002). The reader



should be aware of the potential for this effect to introduce spread in our sample of angular sizes, although it is our expectation that its magnitude will be no greater than the errors in the data set.

### 3.4. Effective Temperature

The stellar effective temperature,  $T_{EFF}$ , is defined in terms of the star’s luminosity and radius by  $L = 4\pi\sigma R^2 T_{EFF}^4$ . Rewriting this equation in terms of angular diameter and bolometric flux, a value of  $T_{EFF}$  was calculated from the flux and Rosseland diameter using

$$T_{EFF} = 2341 \times \left( \frac{F_{BOL}}{\theta_R^2} \right)^{1/4} \quad (2)$$

the units of  $F_{BOL}$  are  $10^{-8}$  erg  $\text{cm}^{-2}\text{s}^{-1}$ , and  $\theta_R$  is in mas. The error in  $T_{EFF}$  is calculated from the usual propagation of errors applied to equation 2. The measured  $T_{EFF}$ ’s are given in column 8 of Table 2, and are found to fall in the range between 2000K and 3250K.

### 3.5. Linear Radius

In order to establish a linear radius from the angular size data presented herein, a distance estimate to the observed Miras needs to be established. Unfortunately, such an estimate can be rather contentious, particularly with the implications upon pulsation mode as can be seen in Haniff, Scholz & Tuthill (1995) and van Belle et al. (1996). Herein we shall consider the infrared period-luminosity relationship of Feast et al. (1989) as considered by Willson (2000). In this review, the relationship is seen to fall in two roughly linear relationships for short and long period Miras, which can be expressed as a function of absolute  $K$  magnitude:

$$M_K = -3.66 \times \log(P) + 1.42 \quad \text{for } P > 400 \quad (3)$$

$$M_K = -6.94 \times \log(P) + 10.0 \quad \text{for } P < 400 \quad (4)$$

The above period-luminosity relationship carries the implicit assumption that all Miras are pulsating in the same mode; given the variability of Miras at  $K$  and other uncertainties in this relationship, we shall assume that distances derived from it have 25% errors. The results which will be established in §4 were also considered in light of the  $K$  band period-luminosity relationship given in Whitelock & Feast (2000) ( $M_K = -3.47 \times \log(P) + 0.84$  for all periods), which favored an overtone pulsation mode, and resulted in only marginal quantitative ( $\approx 4\%$ )

and no qualitative differences in §4. As such, we do not feel that pulsation mode assumptions that might be inherent in the selected period-luminosity relationship affect our conclusions.

Due to the large standard errors in the Hipparcos Mira data set, we will not consider distance metrics derived from the parallaxes for these stars in the otherwise excellent database (eg. van Leeuwen et al. (1997), Whitelock & Feast (2000)). The release of the Hipparcos results (Perryman et al. 1997) has provided the community with a wealth of distance data on a variety of stars. For Miras, however the results were rather unimpressive: the parallaxes showed a great deal of scatter and the standard errors were large (catalog field H16), on average  $2.2 \pm 3.0$  mas for the stars presented in this study, which is consistent with the average standard error of  $2.6 \pm 2.5$  mas found for the 172 M type Miras found in Table 1 of Whitelock & Feast (2000).

There are two potential sources for these effect in the Hipparcos parallax data: First, a 10 mas object (typical of this study) with an intrinsic size of roughly  $350 R_{\odot}$  (van Belle et al. 1997) has a parallax of approximately 3 mas: the angular diameter of a Mira variable is about three times its parallax, with the standard error on a typical parallax being equal to the measurement itself. Determination of a varying visible light photocenter shift, the bandpass of Hipparcos operation, could easily be complicated by this disparity. Second, any spots on the surface of these highly evolved objects could also affect the apparent position of the photocenter (van Leeuwen et al. 1997), although the existence of such spots on Miras has not yet been established empirically. We do not expect this effect to be a function of the typically large distances to the Miras, relative to the majority of stars in the Hipparcos data set. A similar examination of the similarly distant 322 northern hemisphere single (multiplicity field H59 and spectral type both indicating no companions) supergiants found in the Hipparcos dataset indicates a contrasting average standard error of  $0.90 \pm 0.30$  mas; this average standard error appears to be independent of object parallax. Furthermore, the possibility of Lutz-Kelker bias within any given Hipparcos sample of stars has been empirically established (Oudmaijer et al. 1998) and should be carefully considered.

We have detailed our evaluation of the Hipparcos data set at length in this section, given our otherwise positive experience with the catalog’s far-reaching utility. As such, we did not wish to dismiss the Hipparcos Mira data lightly, but did so only after careful consideration of the data.

### 3.6. Re-Analysis of R Cas

One star from van Belle et al. (1996) that bears re-examining is R Cas. In our previous manuscript, a value of  $\theta = 13.55 \pm 0.95$  mas was derived from the measured visibility  $V = 0.1259 \pm 0.0360$  from 4/5 Oct 1995. However, for visibilities below  $V = 0.132$ , the visibility function becomes non-monotonic and has multiple solutions. Neglected in van Belle et al. (1996) were the other angular sizes possible with this visibility: 19.53 and 22.03 mas. The error envelope about the measured visibility encloses the peak of the entire first outlying lobe; hence the error envelope for these angular sizes ranges from 17.90 to 24.16 mas.

Based upon visible light angular size measurements of this object (Haniff, Scholz & Tuthill 1995; Hofmann et al. 2000) that are in the 18 to 36 mas range, the angular size solution most consistent with our previous  $V$  measurement is 22.03 mas. We note, though, that for the visibility measurements outside of the central lobe of the visibility function, the influence of limb darkening and spotting becomes greater and reduces the effectiveness of utilizing single visibility measurements to establish stellar angular sizes, as well illustrated in HSW98.

## 4. Discussion: Size & Pulsation Mode

Theoretical models for many Mira variables predict their effective temperatures will lie at approximately 3,000 to 3,100K, which is somewhat higher than the values seen in Table 2 (cf. Hoffman et al. 1998, Willson 2000). One possible explanation for this discrepancy is a systematic overestimation of the apparent sizes of the variable stars by the interferometer. Absorption of the central star’s flux by molecules will have the effect of contaminating the observed angular sizes and will lead to a  $2.2 \mu\text{m}$  uniform disk size that is markedly larger than the Rosseland mean diameter. A few of the models found in HSW98 show ‘wings’ in the center-to-limb brightness profiles mainly caused by water molecules (Bedding et al. 2001; Jacob & Scholz 2002) that are consistent with this hypothesis, as do all of the dusty Mira models in Bedding et al. (2001). As discussed in §3.3, conversion of the observed interferometric visibility to the desired Rosseland  $\tau = 1$  radius can run afoul of these ‘wings’, causing the inferred size to be dramatically underestimated, as seen in Bedding et al. (2001) and Scholz (2001).

To test this hypothesis, we can examine  $K - [12]$  colors for the Miras observed at IOTA. Twelve micron magnitudes are readily available for these stars, as defined in Hickman, Sloan & Canterna (1995), using flux values for the observed Miras found in the Infrared Astronomical Satellite (IRAS) Point Source Catalog (PSC, 1987).  $K - [12]$  is expected to be

a reasonable indicator of recent dusty mass loss (Le Sidaner & Le Bertre (1996); Beichman et al. (1990)). Given our interest in establishing gross trends in a relative sense between stars of differing  $K - [12]$  values, we did not apply point source corrections to the IRAS  $12\mu\text{m}$  data (Beichman et al. 1988), nor did we attempt to quantify  $12\mu\text{m}$  variability for these sources, which is potentially present in any Mira variable data set (Little-Marenin, Stencel, & Staley 1996; Creech-Eakman 1997), but should in this context only add scatter to the  $12\mu\text{m}$  values.

K band interferometric observations are relatively insensitive to dusty mass loss (though not completely so, as evidenced with VY CMa in Monnier et al. (1999)); however, it is entirely plausible that dusty mass loss will be accompanied by a significant increase in the molecular component of circumstellar material. Significant amounts of absorption by molecules in a circumstellar shell above the Rosseland mean radiating surface will have the effect of increasing the derived size of a interferometrically observed Mira variable. Taking a black body at the expected temperature of 3,000K, the predicted  $K - [12]$  color will be 0.92. By comparison to the observed colors for the individual Miras, we may calculate a  $K - [12]$  excess that will be indicative of stellar mass loss. Given the  $K$  band variability of these objects, we assigned an average error of  $\pm 0.33$  to our derived  $K - [12]$  excess values, which is consistent with the observed K band variability of these objects (Whitelock, Marang & Feast 2000). These data are listed for all the Miras considered in this analysis in Table 3. Examination of our  $K - [12]$  data for R Dra indicates a spurious value, the source of which was unclear. This star was dropped from later consideration in the analysis.

The observed Miras were separated into two sets: those with small values of  $K - [12]$  excess, between 0 and 1.25, which will be indicative of Miras with lower mass loss rates, and those with  $K - [12]$  excess  $> 1.75$ , indicative of the higher mass loss rate Miras; stars in the intermediate  $K - [12]$  range were not considered for this specific analysis (although were a part of analysis associated with Figure 2, later in this section). A plot of this is seen in Figure 1, where the stars with low mass loss show systematically smaller sizes than those with the more substantial mass loss; stars with multiple entries in Table 3 are represented by a corresponding number of data points in Figure 1. Fitting a line to each of the two data sets, we find that  $R = (1.01 \pm 0.50) \times P + (10 \pm 170) R_{\odot}$  for those Miras with little  $K - [12]$  excess (line fit  $\chi^2_{\nu} = 0.41$ ), and  $R = (0.63 \pm 0.64) \times P + (270 \pm 245) R_{\odot}$  for the Miras with  $K - [12]$  excess  $> 1.75$  ( $\chi^2_{\nu} = 0.61$ ). Averaging over periods of 300 to 450 days, we find that the higher mass loss Miras appear on average  $120 R_{\odot}$  (roughly 30%) larger than their lower mass loss counterparts across all periods, with this difference ranging from  $145 R_{\odot}$  to  $90 R_{\odot}$  as the period increases from  $P=275^d$  to  $450^d$ . This correlation of increased radius with  $K - [12]$  excess is a clear indication that the sizes we derive from our interferometric observations progressively overestimate the Rosseland mean diameters for these objects as mass loss increases. Noting the discussion in §3.5, this result is independent of pulsation

mode assumptions.

Furthermore, the direction of that progression appears to indicate that our diameters are systematically biased towards larger sizes, which is consistent with the effects of a circumstellar shell upon the interferometric observables. The presence of circumstellar structures substantial enough to be seen in our interferometric data will grossly invalidate our assumptions regarding interpretation of the visibility data in terms of a scaled uniform disk size, and tend to systematically increase the derived stellar disk size at all spatial frequencies (Bedding et al. 2001; Scholz 2001).

Once we have established  $K - [12]$  color excess dependency for the Mira radii in our sample, we may inspect it to see if there is a correlation between  $K - [12]$  excess and inferred radius, using the inferred radius as a function of period to then inspect the indicated pulsation mode. As discussed in §3.5, the selected period-luminosity relationship has little bearing upon the resultant sizes, and as such, any assumption of pulsation mode inherent in the referenced period-luminosity relationships do not appear to alter our results. For this purpose, we utilized the pulsation mode-dependent radius-period relationships as found in Ostlie & Cox (1986):

$$1.86 \log R = 0.73 \log M + 1.92 + \log P \quad \text{for Fundamental} \quad (5)$$

$$1.59 \log R = 0.51 \log M + 1.60 + \log P \quad \text{for First overtone} \quad (6)$$

Additionally, for the purposes of using this relationship, we shall adopt period-dependent masses, as illustrated in Figure 5 of Willson (2000), with a range of 15% in mass versus period for  $P \leq 400$  days (increasing from 0.7 to 1  $M_{\odot}$  with period), and a range of 25% in mass versus period for  $P > 400$  days (1 to 4  $M_{\odot}$ ). Although this use of a relationship derived from linear, rather than non-linear, modelling might be questionable (Barthes 1998; Ya’ari & Tuchman 1999), it shall be sufficient to establish the dependence of the measured radii upon mass loss rates. Having established these theoretical mode-dependent regions, we may inspect our data in reference to the fundamental and first overtone regions, also seen in Figure 1. There are two striking characteristics to this aspect of the figure. First, the tendency for the Miras with large  $K - [12]$  color excesses to lie in the first overtone region. Second, all of the stars lie above the region defined by the fundamental overtone lines. Both of these aspects are consistent with apparent size overestimation due to circumstellar shell contamination of the visibility data.

Taking the sizes from the Ostlie & Cox (1986) fundamental mode relationship and establishing predicted sizes for all of the stars in our data set, we may plot the observed-to-predicted size ratio versus the  $K - [12]$  excess numbers for all of the Miras in our data set, as seen in Figure 2. There is a clear progression from smaller to larger positive residuals

as the excess increases, with predicted scaling being in excess of 1.0 for all observed stars (excepting R Dra, as noted above). A similar exercise may be carried out in light of the first overtone predictions, but this results in a scaling factor of less than 1.0 for stars with  $K - [12]$  excess less than 1.50, which is more than half of our data set. Scalings less than unity are inconsistent with size enhancement due to circumstellar absorption. It is possible other physical phenomena could appear to decrease the size of the stars when viewed by the interferometer (eg. bright spots), but this explanation is unlikely for two reasons. First, structures at spatial scales smaller than the gross size of the star will need to satisfy a fortuitous geometry to properly affect our visibility data. While this is possible for specific examples in our data set, it seems doubtful that this would present itself as a general effect across our entire ensemble of data. Second, it is unlikely that such structures will have sufficient contrast at  $2.2 \mu\text{m}$  to significantly affect the interferometric observables - for a 10% increase in size, a spot would have to be 33% the diameter of the star, properly aligned, and 1000K hotter than the surrounding photosphere. Both the size and temperature differential of such a spot do not seem credible.

Adjusting the angular diameters by this  $K - [12]$  excess-dependent scaling factor results in the average inferred effective temperature rising from 2500K to 3200K, which is more consistent with the expected effective temperature value for these stars at the Rosseland mean radiating surface when they are pulsating in the fundamental mode (HSW98, Willson (2000)).

Measurements of the angular size of Mira at a variety of wavelengths by other groups appears to support this hypothesis. At  $2.2 \mu\text{m}$ , the  $36.1 \pm 1.4$  mas size measured by Ridgway et al. (1992) is in agreement with a similar recent measurement of 31.6 mas at  $2.26 \mu\text{m}$  by Tuthill et al. (1999b) (no error or phase was given in this promising but preliminary result). However, at  $11.15 \mu\text{m}$ , Weiner et al. (2000) find an angular size of  $47.8 \pm 0.5$  mas. This larger size is consistent with the presence of a circumstellar dust shell, which is in turn consistent with the  $K - [12]$  excess value that we compute to be in excess of 2 magnitudes (see Table 3). Furthermore, Tuthill et al. (1999b) also measured the angular size of Mira at a variety of other wavelengths:  $\theta(1.24\mu\text{m}) = 23.3$  mas,  $\theta(1.65\mu\text{m}) = 28.3$  mas, and  $\theta(3.08\mu\text{m}) = 59.9$  mas. The increased K band size relative to the J band size appears to be consistent with our expectation that the K band sizes are being enhanced by the presence of circumstellar material.

## 5. Conclusions

The IOTA program of observing Mira variable stars has resulted in a substantial increase in the number of near-infrared angular size measurements for Miras; previous results were available for  $\approx 25$  of these stars. Determinations of  $T_{EFF}$  and  $R$  are possible, with the caveat that the derived Rosseland mean radius values are potentially overestimated due to circumstellar shells. The atmospheric models that are utilized in reducing the visibility data clearly play a significant role in the results obtained. Our data are consistent with at least some of the observed Mira variables pulsating in the fundamental mode. For those Miras that appear to be too large to be pulsating in the fundamental mode, there appears to be a correlation between K-[12] color excess and size, reflective of mass loss enhancing the apparent size. If our inference that molecular absorption about the Miras is responsible for an increased apparent K band size of these objects, a number of effects should be observable, the most noticeable of which will be the size of the Miras will appear to be smaller in the J and H bands than in the K band, where such absorption is less. The preliminary results of Tuthill et al. (1999b) appear to support this conclusion. We predict that an angular size pulsation mode study of these objects carried out at  $1.6 \mu\text{m}$  or particularly  $1.2 \mu\text{m}$  will result in unequivocal evidence for fundamental mode pulsation for most if not all Miras.

We would like to thank the staff at the Center for Astrophysics for a generous allotment of telescope time so that this project could be carried out, and Ron Canterna for liberal use of computer resources for data reduction. We acknowledge particularly fruitful discussions with Michael Scholz and Lee Anne Willson. This research has been partially supported by NSF grant AST-9021181 to the University of Wyoming, the Wyoming Space Grant Consortium, and NASA Grant NGT-40050. This research has made use of the SIMBAD database and the AFOEV database, both operated by the CDS, Strasbourg, France. In this research, we have used, and acknowledge with thanks, data from the AAVSO International Database, based on observations submitted to the AAVSO by variable star observers worldwide. Portions of this work were performed at the Jet Propulsion Laboratory, California Institute of Technology under contract with the National Aeronautics and Space Administration.

## REFERENCES

- Alvarez, R., & Mennessier, M.-O. 1997, *A&A*, 317, 761
- Barthes, D., *A&A*, 333, 647
- Bedding, T.R., Jacob, A.P., Scholz, M., Wood, P.R., 2001, *MNRAS*, 325, 1487

- Beichman, C.A., Chester, T., Gillett, F.C., Low, F.J., Matthews, K., Neugebauer, G. 1990, *AJ*, 99, 1569
- Beichman, C.A., Neugebauer, G., Habing, H.J., Clegg, P.E., Chester, T.J., 1988, *IRAS Catalogs and Atlases, Version 2. Explanatory Supplement*, NASA Ref. Publ. 1190
- Bessell, M.S., Scholz, M., Wood, P.R., 1996, *A&A*, 307, 481
- Blackwell, D. E. & Lynas-Gray, A. E. 1994, *A&A*, 282, 899
- Bowen, G.H. 1988, *ApJ*, 329, 299
- Bowen, G. H. & Willson, L. A. 1991, *ApJ*, 375, L53
- Burns, D., et al., 1998, *MNRAS*, 297, 462
- Carleton, N.P. et al. 1994, *Proc. SPIE*, 2200, 152
- Clayton, M.L. & Feast, M.W. 1969, *MNRAS*, 146, 411
- Colavita, M.M., et al. 1999, *ApJ*, 510, 505
- Creech-Eakman, M.J., 1997, Ph.D. thesis, University of Denver
- di Giacomo, A., Lisi, F., Calamai, G., Richichi, A., 1991, *A&A*, 249, 397
- Dyck, H.M., Forbes, F.F., Shawl, S.J., 1971, *AJ*, 76, 901
- Dyck, H.M., Lockwood, G.W. & Capps, R.W. 1974, *ApJ*, 189, 89
- Dyck, H.M. 1995, *AJ*, 109, 378
- Dyck, H.M., Benson, J.A., van Belle, G.T. & Ridgway, S.T. 1996, *AJ*, 111, 1705
- Feast, M.W., Glass, I.S., Whitelock, P.A. & Catchpole, R.M. 1989, *MNRAS*, 241, 375
- Feast, M.W. 1999, in *Asymptotic Giant Branch Stars* (Eds. T. Le Bertre, A. Lebre, and C. Waelkens), TBD
- Fox, M.W. & Wood, P.R., 1982, *ApJ*, 259, 198
- Gerasimovic, B.P., 1928, *Proc. Natn. Acad. Sci. U.S.A.*, 14, 963 (Harv. Reprint 54)
- Gezari, D. Y., Schmitz, M., Pitts, P. S. & Mead, J. M., 1993, *Catalog of Infrared Observations*, NASA Reference Publication 1294



- Groenewegen, M.A.T., 2000, *A&A*, 363, 901
- Groenewegen, M.A.T., Salaris, M., *A&A*, 366, 752
- Haniff, C.A., Ghez, A.M., Gorham, P.W., Kulkarni, S.R., Matthews, K. & Neugebauer, G. 1992, *AJ*, 103, 1662
- Haniff, C.A., Scholz, M. & Tuthill, P.G., 1995, *MNRAS*, 276, 640
- Hickman, M.A., Sloan, G.C., & Canterna, R., 1995, *AJ*, 100, 2910
- Hill, S. J. & Willson, L. A. 1979, *ApJ*, 229, 1029
- Hoffleit, D. 1982, *Catalog of Bright Stars* (Yale University Press, New Haven)
- Hofmann, K.-H., Scholz, M. & Wood, P.R. 1998, *A&A*, 339, 846
- Hofmann, K.-H., Balega, Y., Scholz, M., Weigelt, G., 2000, *A&A*, 353, 1016
- Hofmann, K.-H., Beckmann, U., Blocker, T., Coude du Foresto, V., Lacasse, M., Mennesson, B., Millan-Gabet, R., Morel, S., Perrin, G., Pras, B., Ruilier, C., Schertl, D., Scholler, M., Scholz, M., Shenavrin, V., Traub, W., Weigelt, G., Wittkowski, M., Yudin, B., 2002, *New Astronomy*, 7, 9
- Horne, J.H. & Baliunas, S.L. 1986, *ApJ*, 302, 757
- Hughes, S.M.G. & Wood, P.R., 1990, *AJ*, 99, 784
- IRAS Catalog of Point Sources, Version 2.0, 1987 (GPO & Greenbelt: NASA Astronomical Data Center, Washington, DC) (PSC)
- Jacob, A.P., Scholz, M., 2002, in preparation
- Jura, M. & Kleinmann, S.G. 1992, *ApJS*, 79, 105
- Karovska, M., Nisenson, P., Papaliolios, C. & Boyle, R.P. 1991, *ApJ*, 374L, 51
- Kholopov, P.N., et al. 1988, *General Catalog of Variable Stars*, 4th ed. (Nauka Publishing House, Moscow)
- Lattanzi, M.G., Munari, U., Whitelock, P.A., Feast, M.W. 1997, *ApJ*, 485, 328
- Le Sidaner, P., & Le Berte, P., 1996, *A&A*, 314, 896
- Little-Marenin, I. R., Stencel, R. E., Staley, S. B., 1996, *ApJ*, 467, 806

- Lockwood, G.W. & Wing, R.F. 1971, *ApJ*, 169, 63
- Lockwood, G.W. 1972, *ApJS*, 209, 375
- Mathis, J.S. 1990, *ARA&A*, 28, 37
- Monnier, J.D., Tuthill, P.G., Lopez, B., Cruzalebes, P., Danchi, W.C., Haniff, C.A., 1999, *ApJ*, 512, 351
- Nelson, C.A., Cook, K.H., Popowski, P., Alves, D.R., 2000, *AJ*, 119, 1205
- Neugebauer, G. & Leighton, R.B. 1969, Two-Micron Sky Survey, NASA SP-3047
- Ostlie, D. A. & Cox, A. N. 1986, *ApJ*, 311, 864
- Oudmaijer, R., Groenewegen, M.A.T., Schrijver, H. 1998, *MNRAS*, 294, L41
- Perl, M. & Tuchman, Y. 1990, *ApJ*, 360, 554.
- Perrin, G., et al., 1999, *A&A*, 345, 221
- Perryman, M.A.C., et al. 1997, The Hipparcos and Tycho Catalogs, ESA Sp-1200
- Ribas, I., et al., 2000, *ApJ*, 528, 692
- Ridgway, S.T., Wells, D.C., Joyce, R.R., Allen, R.G., 1979, *ApJ*, 84, 247
- Ridgway, S.T., Benson, J.A., Dyck, H.M., Townsley, L.K., Hermann, R.A., 1992, *AJ*, 104, 2224
- Rowan-Robinson, M. & Harris, S. 1983, *MNRAS*, 202, 767
- Scargle, J.D. 1982, *ApJ*, 263, 835
- Scholz, M. & Takeda, Y. 1987, *A&A*, 186, 200
- Scholz, M., 2001, *MNRAS*, 321, 347
- Schweitzer, E. 1998, Observations from the AFOEV Database, private communication
- Serkowski, K. & Shawl, S.J., 2001, *AJ*, 122, 2017
- Thompson, R.R., Creech-Eakman, M.J., & Akeson, R.L. 2002, *ApJ*, 570, 373
- Thompson, R.R., Creech-Eakman, M.J., & van Belle, G.T. 2002, *ApJ*, in press
- Tuchman, Y., Sack, N. & Barkat, Z. 1979, *ApJ*, 234, 217

- Tuthill, P.G., 1994, Ph.D. dissertation, University of Cambridge
- Tuthill, P.G., Haniff, C.A., Baldwin, J.E., 1999, MNRAS, 306, 353
- Tuthill, P.G., Monnier, J.D., Danchi, W.C., 1999, in Working on the Fringe: Optical and IR Interferometry from Ground and Space, ed. Stephen Unwin and Robert Stachnik, ASP Conference Series Vol. 194, 188
- Tuthill, P.G., Danchi, W.C., Hale, D.S., Monnier, J.D., Townes, C.H., 2000, ApJ, 534, 907
- van Belle, G.T., Dyck, H.M., Benson, J.A., Lacasse, M.G. 1996, AJ, 112, 2147
- van Belle, G.T., Dyck, H.M., Thompson, R.R., Benson, J.A., Kannappan, S.J. 1997, AJ, 114, 2150
- van Belle, G.T. 1999, PASP, 111, 1515
- van Leeuwen, F., Feast, M.W., Whitelock, P.A., Yudin, B., MNRAS, 287, 955
- Weigelt, G., Balega, Y., Hofmann, K.-H., Scholz, M., 1996, A&A, 316, 21
- Weiner, J., Danchi, W.C., Hale, D.D.S., McMahon, J., Townes, C.H., Monnier, J.D., Tuthill, P.G., 2000, ApJ, 544, 1097
- Whitelock, P.A. & Feast, M.W. 2000, MNRAS, 319, 759
- Whitelock, P.A., Marang, F., & Feast, M.W. 2000, MNRAS, 319, 728
- Willson, L. A. & Hill, S. J., 1979 ApJ, 228, 854
- Willson, L.A. 1986, in Late Stages of Stellar Evolution (Eds. S. Kwok & S.R. Pottasch), Reidel Publishing Co., Dordrecht, Holland, 253
- Willson, L.A., Bowen, G.H. & Struck, C. 1996 in From Stars to Galaxies, (Eds. C. Leitherer, U. Fritze-v. Alvensleben & J. Huchra), ASP Conference Series Vol. 98
- Wilson, R.W., Baldwin J.E., Buscher D.F. & Warner P.J. 1992, MNRAS, 257, 369
- Willson, L. A., ARAA, 38 573
- Wood, P. R., 1974, ApJ, 190, 609
- Wood, P. R., 1990, in From Miras to Planetary Nebulae : Which Path for Stellar Evolution?, ed. M.O. Mennessier & A. Omont (Gif-sur-Yvette: Editions Frontières), 67

Wood, P. R., et al., in IAU Symposium #191 : Asymptotic Giant Branch Stars, ed. T. Le Berte, A. Lebre, and C. Waelkens, 151

Wood, P. R., 2000, PASA, 17 18

Ya'ari, A. & Tuchman, Y., ApJ, 514, L35

Young, J.S., et al., 2000, MNRAS, 318, 381

Table 1. The observed data.

Star	Period $P$	$\phi = 0$ JD	Obs. Date	Obs. JD	Phase $\phi$	$B_P$ (m)	$V^a$	$\theta_{UD}$ (mas)
RR Aql	399.8	50,046	96-Jun-04	50239	0.48	31.13	0.465	$10.73 \pm 0.66$
RT Aql	328.6	49,875	96-Jun-03	50238	0.10	37.00	0.705	$7.24 \pm 0.42$
			96-Jun-07	50242	0.12	35.45	0.582	
V Cam	524.5	50,190	96-Oct-09	50366	0.34	26.57	0.759	$8.36 \pm 0.40$
			96-Oct-09	50366	0.34	27.41	0.740	
			96-Oct-09	50366	0.34	28.04	0.663	
			96-Oct-09	50366	0.34	28.64	0.692	
V Cas	226.6	50,289	96-Oct-06	50363	0.33	34.69	0.740	$6.30 \pm 0.66$
Y Cas	410.7	50,303	96-Oct-07	50364	0.15	35.95	0.643	$7.28 \pm 0.59$
S CrB	359.5	49,725	96-Mar-07	50150	0.18	21.21	0.754	$11.35 \pm 0.26$
			96-Mar-07	50150	0.18	21.21	0.662	
			96-Mar-07	50150	0.18	21.21	0.726	
			96-Mar-08	50151	0.19	21.21	0.663	
			96-Mar-08	50151	0.19	21.21	0.641	
			96-Mar-08	50151	0.19	21.21	0.639	
			96-Mar-08	50151	0.19	21.21	0.619	
			96-Mar-08	50151	0.19	21.21	0.611	
			96-Mar-08	50151	0.19	21.21	0.555	
			96-Mar-08	50151	0.19	21.20	0.598	
			96-Mar-12	50155	0.20	38.22	0.357	
			96-Mar-12	50155	0.20	38.21	0.368	
R CVn	329.2	50,150	96-Mar-13	50156	0.02	37.00	0.681	$6.63 \pm 0.59$
			96-May-29	50233	0.25	37.60	0.583	$7.66 \pm 0.28$
			96-May-30	50234	0.26	37.57	0.590	
			96-May-30	50234	0.26	37.66	0.599	
			96-Jun-07	50242	0.28	35.52	0.581	
BG Cyg	287.7	49,524	96-Jun-07	50242	0.50	35.45	0.877	$4.14 \pm 0.83$
DG Cyg	463.9	49,891	96-May-29	50233	0.74	36.80	0.784	$5.36 \pm 0.66$
R Dra	246.0	50,431	97-Jul-05	50635	0.83	20.90	0.658	$12.04 \pm 1.36$
			97-Jul-05	50635	0.83	20.57	0.692	
RU Her	485.6	49,800	96-Jun-02	50237	0.90	37.58	0.507	$8.71 \pm 0.39$
			96-Jun-03	50238	0.90	37.57	0.457	
U Her	406.4	49,880	96-Jun-02	50237	0.88	37.31	0.263	$11.18 \pm 0.60$
R LMi	372.8	49,600	96-Mar-07	50150	0.48	21.19	0.534	$14.40 \pm 0.66$
			96-Mar-07	50150	0.48	21.19	0.668	
			96-Mar-07	50150	0.48	21.07	0.529	
			96-Mar-07	50150	0.48	21.05	0.552	
RT Oph	427.4	49,925	96-Jun-07	50242	0.74	35.16	0.717	$6.52 \pm 0.64$
UU Peg	458.5	49,690	96-Jun-03	50238	0.20	36.96	0.417	$9.56 \pm 0.56$
Z Peg	331.4	50,711	96-Oct-04	50361	0.94	37.64	0.838	$4.50 \pm 0.71$
RR Per	390.1	50,039	96-Oct-07	50364	0.83	35.99	0.679	$6.83 \pm 0.61$
U Per	317.5	50,165	96-Oct-06	50363	0.62	33.93	0.811	$5.41 \pm 0.75$
BG Ser	394.8	48,450	96-Jun-04	50239	0.53	30.51	0.769	$6.71 \pm 0.78$
S Ser	375.9	49,875	96-Mar-11	50154	0.74	36.98	0.733	$5.51 \pm 0.42$
			96-Mar-11	50154	0.74	36.89	0.796	
			96-Mar-11	50154	0.74	36.89	0.796	
			96-Jun-08	50243	0.98	32.26	0.832	$5.35 \pm 0.82$
S UMi	328.2	49,850	96-Jun-06	50241	0.19	26.67	0.752	$7.98 \pm 0.87$

Table 1—Continued

Star	Period $P$	$\phi = 0$ JD	Obs. Date	Obs. JD	Phase $\phi$	$B_P$ (m)	$V^a$	$\theta_{UD}$ (mas)
RS Vir	354.1	49,325	96-Jun-10	50245	0.60	32.38	0.683	$7.54 \pm 0.67$
R Cas <sup>b</sup>	430.8	50,940	95-Oct-4	49995	0.81	35.27	0.125	$22.03^{+2.13}_{-4.13}$
			95-Oct-5	49996	0.81	36.30	0.1273	

<sup>a</sup>Standard nightly error is  $\Delta V = 0.0509$ .

<sup>b</sup>R Cas data is reanalysis of visibility data from van Belle et al. (1996).

Table 2. Derived parameters: bolometric flux, Rosseland angular diameter, effective temperature, distance and linear radius.

Star	Date	$V$	$K$	$V - K$	$F_{BOL}$ $10^{-8}$ erg cm <sup>-2</sup> s <sup>-1</sup>	$\theta_R$ (mas)	$T_{EFF}$ (K)
RR Aql	96-Jun-04	12.8	$0.65 \pm 0.11$	$12.1 \pm 0.5$	$78.4 \pm 11.8$	$10.73 \pm 0.79$	$2127 \pm 111$
RT Aql	96-Jun-03	9.5	$0.50 \pm 0.12$	$9.0 \pm 0.5$	$101.7 \pm 15.2$	$7.24 \pm 0.51$	$2763 \pm 125$
V Cam	96-Oct-09	13.0	$0.63 \pm 0.10$	$12.4 \pm 0.5$	$79.1 \pm 11.9$	$8.36 \pm 0.52$	$2414 \pm 86$
V Cas	96-Oct-06	10.8	$1.88 \pm 0.20$	$8.9 \pm 0.6$	$28.6 \pm 4.3$	$6.30 \pm 0.71$	$2157 \pm 146$
Y Cas	96-Oct-07	11.2	$0.47 \pm 0.20$	$10.7 \pm 0.6$	$97.4 \pm 14.6$	$7.28 \pm 0.66$	$2727 \pm 160$
S CrB	96-Mar-07	10.4	$-0.07 \pm 0.03$	$10.5 \pm 0.4$	$160.5 \pm 24.1$	$11.35 \pm 0.52$	$2473 \pm 46$
R CVn	96-Mar-13	8.5	$0.01 \pm 0.46$	$8.5 \pm 0.8$	$134.8 \pm 20.2$	$7.66 \pm 0.41$	$2882 \pm 90$
	96-May-29	10.5	$0.14 \pm 0.05$	$10.4 \pm 0.4$	$162.9 \pm 24.4$	$6.63 \pm 0.64$	$3248 \pm 200$
BG Cyg	96-Jun-07	11.5	$1.05 \pm 0.12$	$10.5 \pm 0.5$	$57.9 \pm 8.7$	$4.14 \pm 0.84$	$3175 \pm 344$
DG Cyg	96-May-29	11.0	$1.18 \pm 0.20$	$9.8 \pm 0.6$	$52.6 \pm 7.9$	$5.36 \pm 0.69$	$2723 \pm 204$
R Dra	97-Jul-05	11.3	$0.66 \pm 0.14$	$10.6 \pm 0.5$	$82.6 \pm 12.4$	$12.04 \pm 1.44$	$2034 \pm 139$
RU Her	96-Jun-02	11.3	$0.25 \pm 0.12$	$11.0 \pm 0.5$	$114.7 \pm 17.2$	$8.71 \pm 0.52$	$2596 \pm 109$
U Her	96-Jun-02	10.3	$-0.04 \pm 0.13$	$10.3 \pm 0.5$	$158.9 \pm 23.8$	$11.18 \pm 0.75$	$2486 \pm 125$
R LMi	96-Mar-07	13.0	$-0.16 \pm 0.06$	$13.2 \pm 0.4$	$158.6 \pm 23.8$	$14.40 \pm 0.87$	$2189 \pm 87$
RT Oph	96-Jun-07	14.0	$2.03 \pm 0.50$	$12.0 \pm 0.8$	$22.1 \pm 3.3$	$6.52 \pm 0.69$	$1989 \pm 129$
UU Peg	96-Jun-03	13.8	$0.82 \pm 0.15$	$12.9 \pm 0.5$	$64.9 \pm 9.7$	$9.56 \pm 0.68$	$2149 \pm 111$
Z Peg	96-Oct-04	9.3	$1.24 \pm 0.20$	$8.0 \pm 0.6$	$53.7 \pm 8.0$	$4.50 \pm 0.73$	$2987 \pm 267$
RR Per	96-Oct-07	13.1	$1.50 \pm 0.20$	$11.6 \pm 0.6$	$36.5 \pm 5.5$	$6.83 \pm 0.66$	$2202 \pm 135$
U Per	96-Oct-06	9.3	$1.05 \pm 0.20$	$8.2 \pm 0.6$	$63.3 \pm 9.5$	$5.41 \pm 0.78$	$2839 \pm 230$
BG Ser	96-Jun-04	11.9	$0.38 \pm 0.19$	$11.5 \pm 0.5$	$103.1 \pm 15.5$	$6.71 \pm 0.83$	$2879 \pm 207$
S Ser	96-Mar-11	11.8	$2.03 \pm 0.26$	$9.8 \pm 0.6$	$26.9 \pm 4.0$	$5.35 \pm 0.84$	$2305 \pm 201$
	96-Jun-08	11.8	$2.03 \pm 0.45$	$9.8 \pm 0.7$	$24.1 \pm 3.6$	$5.51 \pm 0.48$	$2209 \pm 106$
S UMi	96-Jun-06	10.2	$-0.09 \pm 0.15$	$10.3 \pm 0.5$	$166.4 \pm 25.0$	$7.98 \pm 0.93$	$2977 \pm 206$
RS Vir	96-Jun-10	13.2	$1.36 \pm 0.20$	$11.8 \pm 0.6$	$41.2 \pm 6.2$	$7.54 \pm 0.74$	$2160 \pm 133$
R Cas <sup>a</sup>	95-Oct-4	11.1	$-1.29 \pm 0.13$	$12.4 \pm 0.4$	$447.4 \pm 85.2$	$23.03^{+2.13}_{-4.13}$	$2239^{+152}_{-236}$

<sup>a</sup>R Cas data is reanalysis of visibility data from van Belle et al. (1996).

Table 3. Mira variable absolute K magnitudes, distances, radii, IRAS  $12\mu\text{m}$  magnitudes,  $K - [12]$  colors, and estimated  $K - [12]$  color excesses.

Star	Date	$M_K$ (mag)	dist (pc)	Radius ( $R_\odot$ )	[12] (mag)	$K - [12]$ (mag)	$K - [12]$ excess (mag)	Ref
R Aql	95-Jun-10	-7.55	224	$259 \pm 67$	-2.88	2.04	1.13	1
	95-Oct-06	-7.55	224	$328 \pm 85$	-2.88	2.11	1.20	1
RR Aql	96-Jun-04	-8.09	561	$648 \pm 169$	-2.67	3.32	2.41	2
RT Aql	96-Jun-05	-7.46	392	$305 \pm 79$	-1.05	1.55	0.64	2
R Aqr	95-Jul-11	-8.05	272	$438 \pm 114$	-4.37	3.36	2.45	1
	95-Oct-07	-8.05	272	$412 \pm 106$	-4.37	3.63	2.72	1
U Ari	77-Sep-03	-7.98	779	$801 \pm 205$	-0.99	2.47	1.56	3
R Aur	95-Oct-03	-8.46	342	$407 \pm 105$	-3.03	2.24	1.33	1
V Cam	96-Oct-09	-8.87	796	$716 \pm 185$	-2.14	2.77	1.86	2
R Cas	95-Oct-04	-8.28	250	$593 \pm 181$	-4.19	2.90	1.99	2
T Cas	95-Oct-04	-8.38	302	$416 \pm 108$	-2.95	1.97	1.06	1
V Cas	96-Oct-06	-7.33	696	$472 \pm 129$	-0.94	2.82	1.91	2
Y Cas	96-Oct-07	-8.14	527	$413 \pm 110$	-1.34	1.82	0.91	2
<i>o</i> Cet	90-Aug-21	-7.80	121	$482 \pm 124$	-5.59	3.39	2.48	4
	90-Sep-19	-7.80	121	$468 \pm 120$	-5.59	2.99	2.08	4
S CrB	96-Mar-08	-7.93	375	$457 \pm 116$	-2.13	2.07	1.16	2
R CVn	96-Mar-13	-7.79	391	$279 \pm 75$	-1.40	1.41	0.50	2
	96-May-31	-7.79	391	$322 \pm 82$	-1.40	1.74	0.83	2
BG Cyg	96-Jun-07	-7.57	530	$236 \pm 76$	-0.74	1.79	0.88	2
DG Cyg	96-May-29	-8.50	865	$499 \pm 140$	...	...	...	2
R Dra	97-Jul-05	-7.32	395	$511 \pm 142$	0.42	0.24	-0.67	2
RU Her	96-Jun-02	-8.64	610	$572 \pm 147$	-1.97	2.25	1.34	2
S Her	95-Jul-07	-7.68	677	$354 \pm 124$	-0.21	1.68	0.77	1
U Her	95-Jun-10	-8.11	377	$431 \pm 114$	-3.12	2.69	1.78	1
	96-Jun-02	-8.11	377	$453 \pm 117$	-3.12	3.08	2.17	2
R Leo	90-May-02	-7.81	115	$409 \pm 105$	-4.71	2.21	1.30	5
R LMi	96-Mar-07	-7.98	367	$569 \pm 146$	-2.94	2.78	1.87	2
RT Oph	96-Jun-07	-8.26	1,142	$801 \pm 217$	-0.80	2.83	1.92	2
X Oph	95-Jul-07	-7.80	225	$314 \pm 81$	-2.90	1.87	0.96	1
	95-Oct-07	-7.80	225	$298 \pm 78$	-2.90	1.85	0.94	1
S Ori	95-Jul-07	-8.30	481	$545 \pm 142$	-1.82	1.93	1.02	1
U Ori	95-Oct-08	-7.98	310	$370 \pm 96$	-3.45	2.93	2.02	1
R Peg	95-Jul-07	-8.00	435	$476 \pm 122$	-2.03	2.53	1.62	1
	95-Oct-06	-8.00	435	$455 \pm 119$	-2.03	1.85	0.94	1
S Peg	95-Oct-06	-7.74	675	$459 \pm 135$	-0.37	1.82	0.91	1
	95-Jul-08	-7.74	675	$574 \pm 154$	-0.37	1.73	0.82	1
UU Peg	96-Jun-03	-8.47	721	$742 \pm 193$	-1.89	2.71	1.80	2
Z Peg	96-Oct-04	-7.80	640	$310 \pm 92$	-0.70	1.93	1.02	2
RR Per	96-Oct-07	-8.06	816	$599 \pm 161$	-0.76	2.26	1.35	2
U Per	95-Oct-04	-7.73	559	$352 \pm 101$	-0.66	1.63	0.72	1
	96-Oct-06	-7.73	559	$325 \pm 94$	-0.66	1.71	0.80	2
BG Ser	96-Jun-04	-8.07	491	$354 \pm 99$	-1.56	1.94	1.03	2
R Ser	95-Jul-07	-7.91	356	$328 \pm 86$	-2.07	1.92	1.01	1
S Ser	96-Mar-11	-8.00	1,012	$601 \pm 159$	-0.45	2.48	1.57	2
	96-Jun-08	-8.00	1,012	$583 \pm 172$	-0.45	2.48	1.57	2
S UMi	96-Jun-06	-7.78	345	$296 \pm 82$	-1.78	1.69	0.78	2
RS Vir	96-Jun-10	-7.90	712	$577 \pm 155$	-1.46	2.82	1.91	2

References. — 1. van Belle et al. (1996), 2. van Belle et al. (2002), 3. Ridgway et al. (1979), 4. Ridgway et al. (1992), 5. di Giacomo et al. (1991).

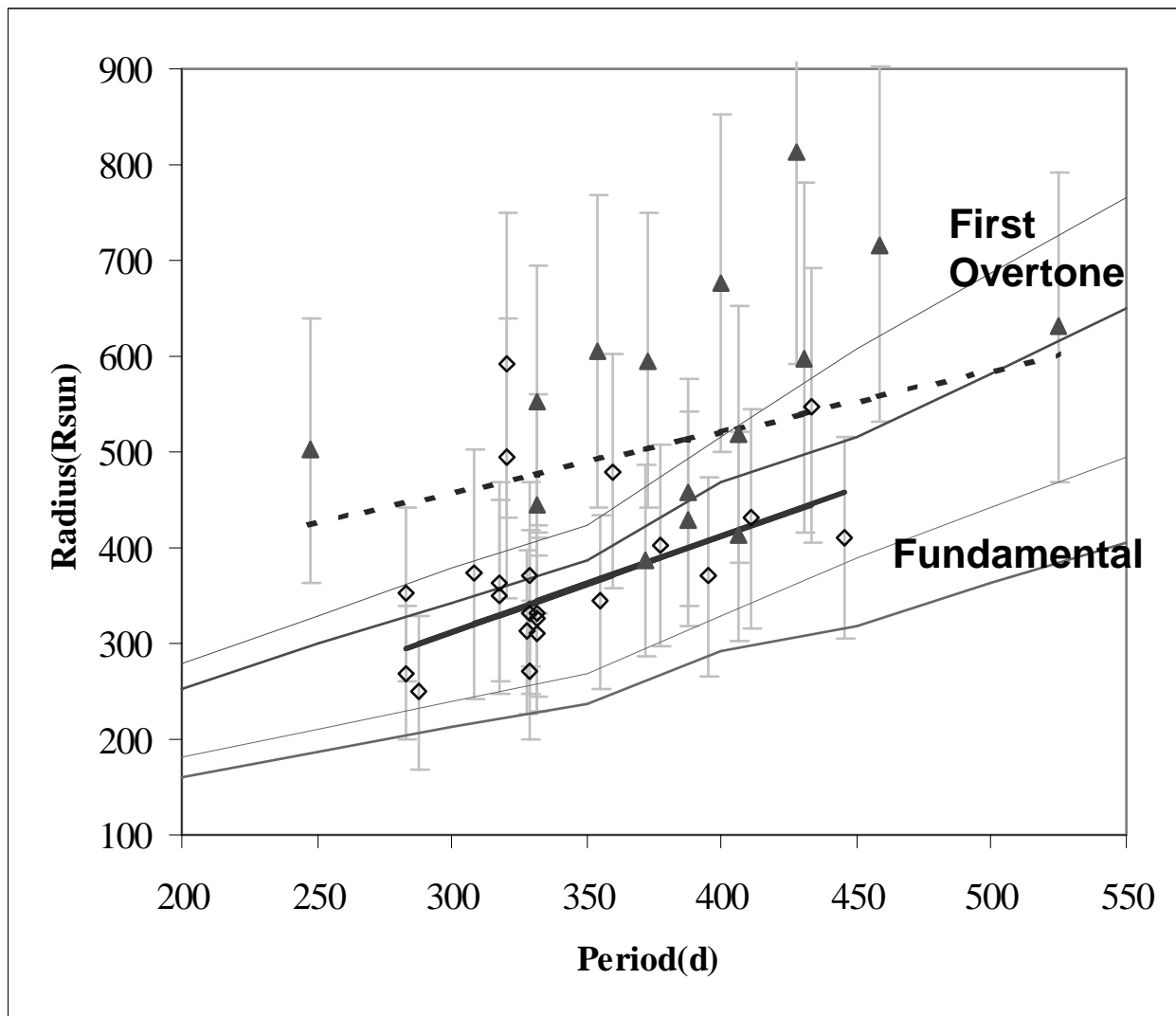


Fig. 1.— Radius versus period for the Miras observed. Open diamonds are for Miras with  $K - [12]$  excess between +0.0 and +1.25, indicating less dusty mass loss, and filled triangles are for Miras with  $K - [12]$  excess  $> +1.75$ , indicating more mass loss. Comparing fit lines for the lower and higher mass loss Miras (solid and dotted, respectively), the Miras with greater dusty mass loss appear on average  $120 R_{\odot}$  larger. The fundamental and first overtone regions are derived from the radius-period relationships found in Ostlie & Cox (1986). See §4 for details of the line fits.



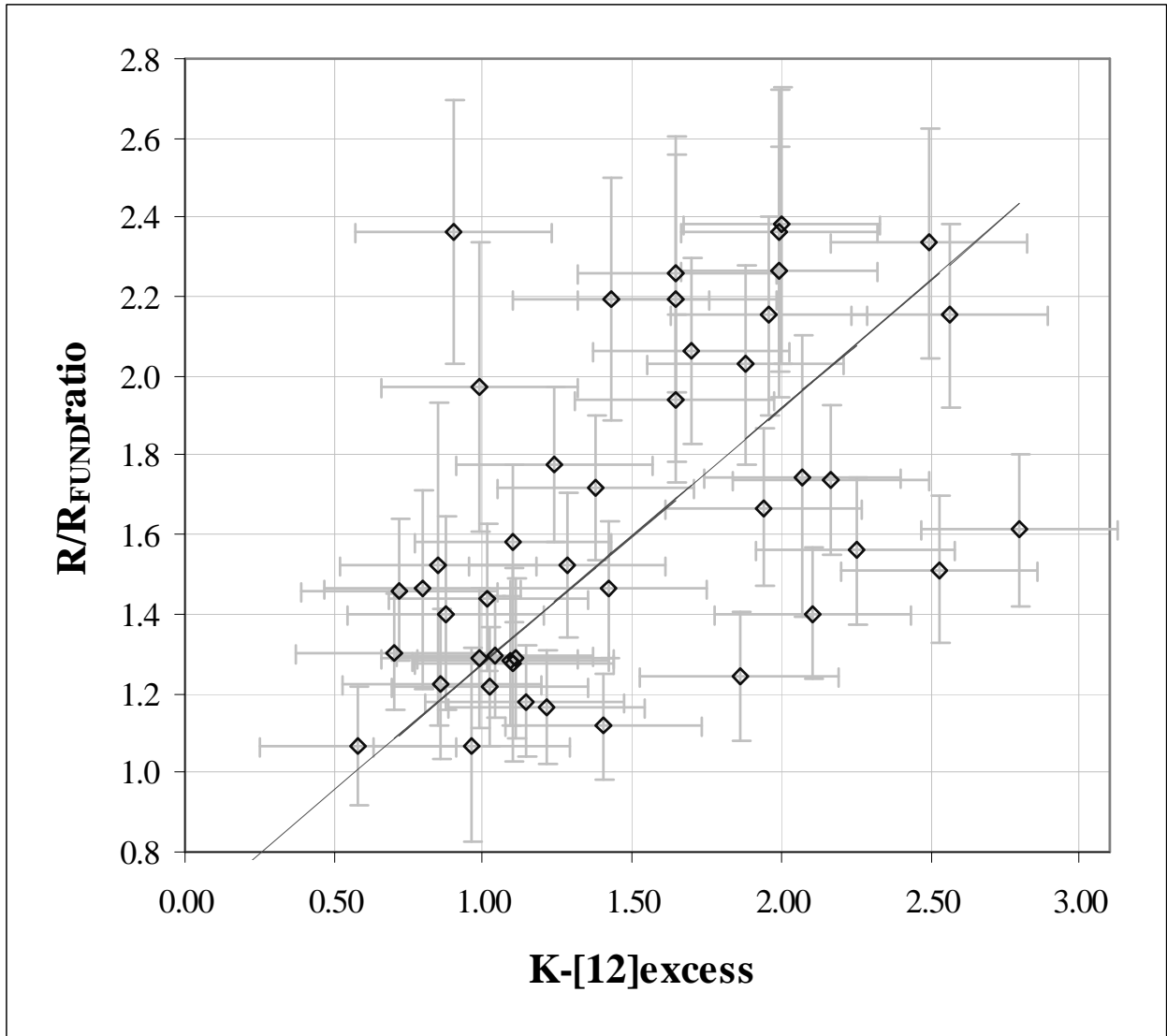


Fig. 2.— Ratio of observed radius to predicted fundamental mode radius versus  $K - [12]$  excess.